1st International Conference on 3D Materials Science
Edited by: Marc De Graef, Henning Friis Poulsen, Alexis Lewis, Jeff Simmons, George Spanos
TMS (The Minerals, Metals & Materials Society), 2012

3D CHARACTERIZATION OF RECRYSTALLIZATION BOUNDARIES

Yubin Zhang[1], Andrew Godfrey[2], Nicole MacDonald[3], Dorte Juul Jensen[1]

[1] Danish-Chinese Center for Nanometals, Materials Science and Characterization Section, Institute of Wind Energy, Technical University of Denmark, DK-4000 Roskilde Denmark
[2] Laboratory of Advanced Materials, Department of Materials Science and Engineering, Tsinghua University, Beijing 100084, P.R. China
[3] Center for Electron Nanoscopy, Technical University of Denmark, DK-2800 Kongens Lyngby, Denmark

Keywords: grain boundary, recrystallization, aluminum, protrusion/retrusion

Abstract

A three-dimensional (3D) volume containing a recrystallizing grain and a deformed matrix in a partially recrystallized pure aluminum was characterized using the 3D electron backscattering diffraction technique. The 3D shape of a recrystallizing boundary, separating the recrystallizing grain and deformed matrix, was reconstructed. The result shows a very complex structure containing several large protrusions and retrusions. A correlation between the protrusions/retrusions and the deformed matrix in front of the boundary shows that the deformed microstructure has a very strong influence on the formation of protrusions/retrusions.

Introduction

The migration of recrystallizing boundaries is important for the recrystallization process and, as a result, the recrystallization texture [1]. Microstructural characterization using electron microscopy and three-dimensional x-ray diffraction (3DXRD) have shown that the recrystallizing boundary and its migration are very inhomogeneous: a recrystallizing boundary migrates generally in a stop-go fashion, and consists of many protrusions and retrusions on a local scale [2-4]. Ex situ and in situ investigations [5,6] of the migration of individual recrystallizing boundaries have revealed that the formation of pro-/re-trusions may be important for the migration of recrystallization boundaries and can partly explain the observed stop-go motion. More recently phase-field model simulations [7] have provided evidence to suggest that the existence of pro-/re-trusions can lead to an increase in the migration velocity compared to a flat boundary.

Clear observations of pro-/re-trusions can be traced back to the classical work of Beck and Sperry from the 1950's [8]. However, only in the past few years, after the publication of in situ 3DXRD experiments [2] have detailed investigations focusing on these local features been reported [3-7,9-11]. These include several simulation methods: molecular dynamic simulations [12,13], phase-field simulations [7], and numerical analysis [10,11], all of which have been used to investigate the effects of heterogeneity in the deformed microstructure on the formation of pro-/re-trusions. Due to the fact that highly idealized microstructures have been used in all these simulations, none of these approaches can be applied directly for the interpretation of experimental data, because large and non-regular heterogeneities exist in the deformed matrix.

The results of previous 2D investigations suggest that the average size of pro-/re-trusions cannot simply be correlated with the stored energy in the deformed microstructure in front of recrystallizing boundary [5, 9]. It has also been suggested however that in order to fully understand the formation of pro-/re-trusions, the microstructure in the third dimension (i.e. below observed surface) also needs to be considered, because i) the mobility of the recrystallizing

boundary may depend on the boundary plane, and ii) the deformed microstructure in the third dimension may affect the formation of pro-/re-trusions [6, 9]. The present study is therefore focused on characterization of a recrystallizing boundary and the neighboring deformed microstructure in 3D.

Experiment

The material used for this study was 99.996% pure aluminum. The material was first annealed at 550°C for 24h to obtain a grain size of several millimeters, followed by cold rolling to 50% reduction in thickness. The deformed samples were annealed at 250°C for 10 minutes to obtain partially-recrystallized microstructures. After grinding using silicon carbon paper down to 4000 followed by mechanical polishing to 1µm, the specimen was electropolished on the longitudinal sections (defined by the sample rolling direction (RD) and normal direction (ND)) in a Struers A2 solution.

3D-EBSP mappings were carried out using an FEI Helios Nanolab 600 DualBeam^{TM} platform consisting of focused ion beam (FIB) and field emission gun SEM (FEGSEM) columns, and interfaced with a TSL^{TM} EBSP facility (details of these techniques can be found in [14,15]). The recrystallizing boundary was by chance near one of the sample edges which was parallel to ND (see Figure 1), which minimized the milling work required to alleviate problems with shadowing during the EBSP mapping. Before the 3D serial sectioning was performed, the adjoining perpendicular rough surface, which was not electropolished, and which was connected to this edge on the transverse plane (defined by ND and the transverse direction (TD)) was cleaned using FIB by making a rough cut with a current of 20nA, followed by a final polishing with a current of 2nA. A ~1µm layer of Pt was then deposited on this surface (facing the ion beam during serial sectioning) to minimize damage from the ion beam (see Figure 1). A fiducial mark was also made on this surface next to the platinum layer, and this was used to automatically align the sample during the serial sectioning. An in-house computer program was used for the automated movement of the sample between consecutive FIB milling and EBSP mapping steps. The sample was consecutively milled perpendicular to the Pt layer using an accelerating voltage and current of 30kV and 2nA, respectively. Each milling stage removed a layer of material of 0.5 µm in thickness. In total 40 milled surfaces on the ND-RD section were mapped by EBSP using an electron beam step size, accelerating voltage and probe current of 0.5µm, 15kV and 2.1nA, respectively. During scanning the Pt layer was also mapped, and appeared as lines consisting of non-indexed points in the EBSP maps, which are ideal features for the post-mapping alignment of the EBSP maps.

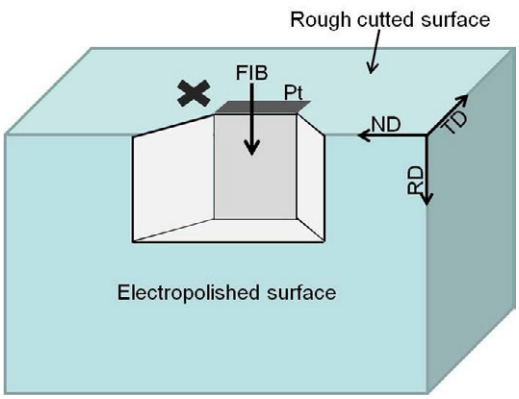

Figure1. Sketch of sample showing the geometry of milling and EBSP mapping

Result and discussion

An EBSP map of the microstructure of a typical RD-ND section, together with its {111} pole figure is shown in Figure 2. The color code in this map is based on the RD inverse pole figure. A recrystallizing boundary consisting of several pronounced pro-/re-trusions separates the recrystallizing grain and the deformed matrix. In the deformed matrix, two set of intersecting boundaries, inclined about ±35°to RD, can be clearly seen. This is a typical deformed microstructure after medium strain deformation and some recovery of pure aluminum [16,17].
On the bottom of the map, a region corresponding to the Pt layer (see Figure 1) is seen, and this was used as the reference for sample alignment. During alignment, the rotation between any two neighboring layers was ignored and only the translation along RD was considered.
The 3-D reconstructed microstructure consisting of the 40 sections is shown in Figure 2c, in which the reconstructed RD-TD and ND-TD sections can be seen. The bands seen in the RD-ND section continue along TD and are nearly parallel to TD. This has also been reported in TEM observations [18, 19]. The pro-/re-trusions on the RD-TD section are on average more flat than those on the RD-ND section.

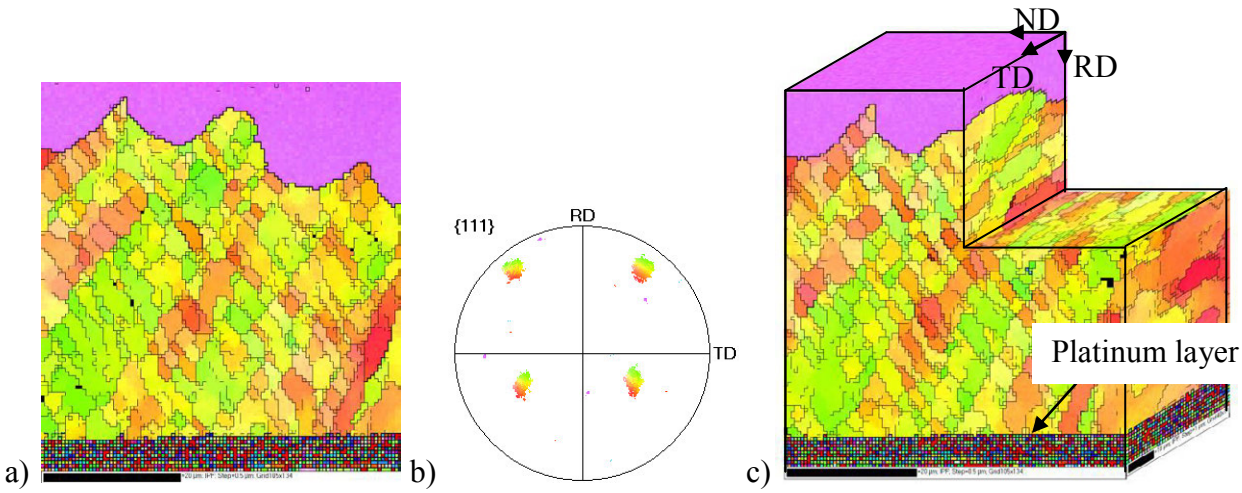

Fig. 2 EBSP map showing a typical section of the microstructure seen in a RD-ND section a) and its corresponding pole figure b); c) 3D volume showing the reconstructed microstructure.

In order to see the 3D shape of the recrystallizing boundaries, a subset of the deformed matrix in each slice was extracted from the EBSP maps, and a 3D volume of the deformed microstructure was reconstructed. In Figure 3 two different views of the reconstructed deformed microstructure are shown, in which the reconstructed top surface of this volume represents the 3D shape of the recrystallizing boundary, showing clearly heterogeneity of the pro-/re-trusions in different sample directions. It is interesting to note that in 3D the pro-/re-trusions are not isolated peaks but elongated ridges along TD. There are also some areas which are rather flat, which is in agreement with the 3DXRD observations [20] and the analysis of facet migration [4].

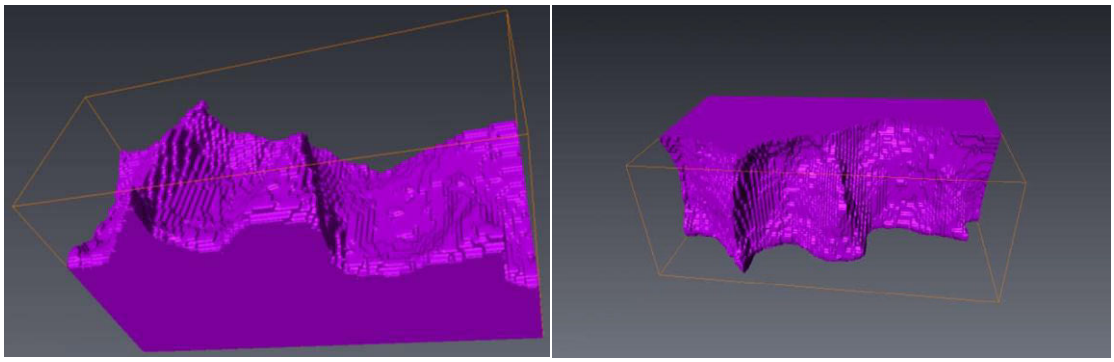

Figure 3. Two views of the recrystallizing boundary surface; the solid purple volume is the deformed matrix.

The EBSP maps contain also orientation information, from which the misorientation across the recrystallizing boundary can be obtained. Figure 4 shows the same 3D recrystallizing boundary in a new way using colors which represent the misorientations across the boundary at each location. The corresponding misorientation rotation axes and angles for all pixels on the boundary are also shown in the inverse pole figure and color bar, respectively.

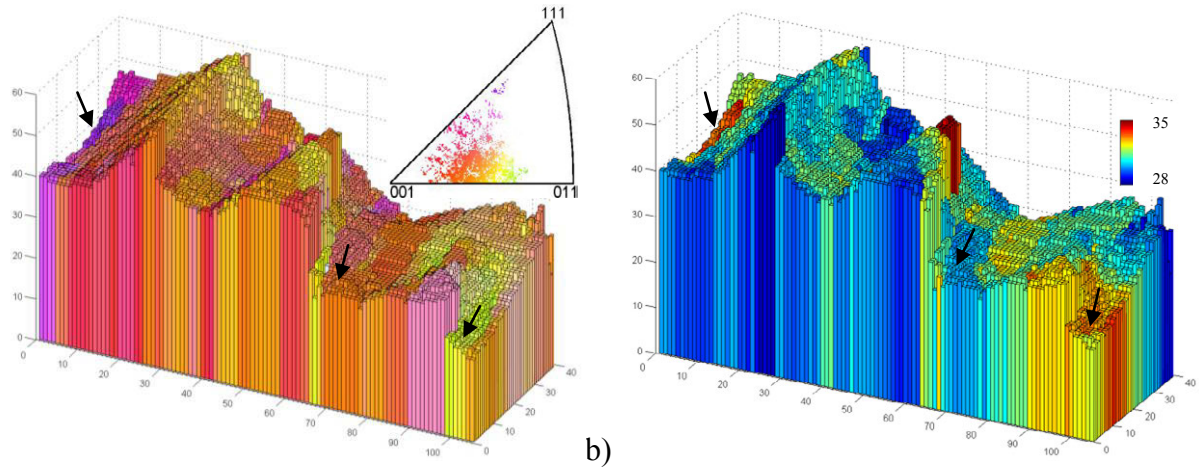

a) b)

Figure 4. The 3D recrystallizing boundary shown in different colors which are converted from the misorientation rotation axes a) and angles b). The color code for the misorientation rotation axis is the same as that used in inverse pole figure (see insert to Figure 4a), while for the misorientation angle a linear color code from blue to red was used (see insert to Figure 4b).

It can be seen that the colors (hence misorientations) at the protrusions are quite mixed. For example, the protrusions marked by black arrows have wide range of misorientation rotation axes (purple, light green or orange in the figure), and the misorientation angles can be either low or high. Similar observations are found for the boundary segments on the retrusions. Moreover, there appears to be also no systematic difference in color between the boundary segments on the protrusions and on the retrusions. This implies that there is only a relatively small difference in misorientation between segments on protrusions and on retrusions. However, it should be stressed that this does not mean that the local mobility has no effect on the formation of pro-/re-trusions. The mobility depends not only on the misorientation but also on the boundary plane, and this needs to be further analyzed before conclusions can be drawn.

Boundary pinning at solutes or second-phase particles, which is often seen in alloys, cannot be ruled out with regard to the formation of pro-/re-trusions. However, based on the frequency with which pro-/re-trusions are seen in ultra pure, normal purity and less pure materials, it is suggested that the heterogeneity in the deformed microstructure may be the main reason for the formation of protrusions/retrusions in pure materials.
In the deformed matrix, the dislocation boundaries on RD-TD section are elongated along TD and are more or less parallel to TD (Figure 2c). Two examples of extended band structures subtracted from the deformed matrix are shown in Figure 5, where 2° is used to detect dislocation boundaries. In both cases the whole band of dislocation structure is more or less parallel to TD. Figure 5 therefore clearly shows that the actual 3D bands in the deformed microstructure can reasonably be represented as by the 2D microstructure on RD-ND section. The 3D shape of the recrystallizing boundary (Figure 3) also shows a little variation along TD. This clearly indicates that the extended band deformation structure along TD has a strong influence on the 3D shape of pro-/re-trusions.

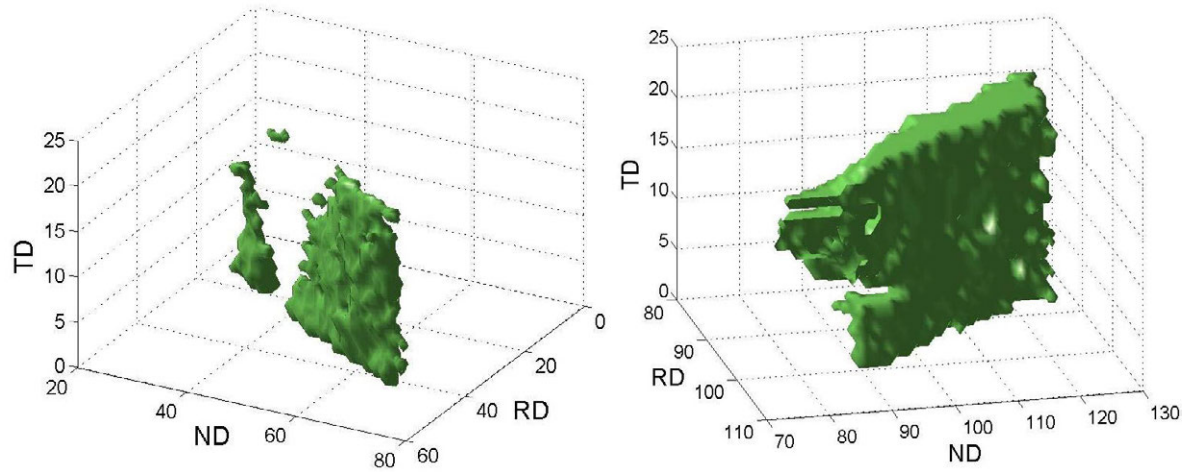

Figure 5. Two examples showing the 3D band structure in the deformed matrix.

It is important to point out that the deformed microstructure which has induced the formation of pro-/re-trusions that is seen in the microstructure, is the one which has already been ‘eaten’ at this stage. Therefore, it would be very interesting to perform experiments to observe in-situ the recrystallizing grain growing into variously oriented deformed matrices in full 3D, where the true correlation between deformed matrix and pro-/re-trusions can be obtained.

Summary

In the present paper a 3D recrystallizing boundary and the deformed matrix in front of the boundary has been characterized using the 3D EBSP technique. The results show that the recrystallizing boundary has a very complex shape in 3D, consisting of large protrusions and retrusions. The pro-/re-trusions are more pronounced on the RD-ND section than on the RD-TD section. It has also been found that the deformed matrix has a strong influence on the formation of protrusion and retrusions.

Acknowledgement

The authors gratefully acknowledge support from the Danish National Research Foundation and the National Natural Science Foundation of China (Grant No. 50911130230) for the Danish-Chinese Center for Nanometals, within which this work was performed.

References:

1. F. Haessner, *Recrystallization of metallic materials*. (Dr. Riederer Verlag GmbH Stuttgart, 1978).
2. S. Schmidt et al., "Watching the growth of bulk grains during recrystallization of deformed metals, " *Science*, 305(2004), 229-232.
3. Y.B. Zhang et al., "Analysis of the growth of individual grains during recrystallization in pure nickel, " *Acta Mater.* 2009;57: 2631-2639.
4. S. Van Boxel et al., "Monitoring grain boundary migration during recrystallisation using topotomography, " *Proceeding of the 31st Risø International Symposium* (2010), 449-456.
5. Y.B. Zhang, A. Godfrey, D. Juul Jensen, "Local boundary migration during recrystallization in pure aluminum, " *Scripta Mater.* 64(2011), 331-334.
6. Y.B. Zhang, A. Godfrey, D. Juul Jensen, "In-situ observations of migration of recrystallization boundaries in pure aluminium," *Proceeding 31st Risø International Symposium.* (2010), 497-503.
7. N. Moelans et al., to be submitted for publication.
8. P.A. Beck, P.R. Sperry, H. Hu. "The orientation dependence of the rate of grain boundary migration," *J Appl Phys* 21(1950),420-425.
9. Y.B. Zhang, A. Godfrey, D. Juul Jensen, "Measurements of the Curvature of Protrusions/Retrusions on Migrating Recrystallization Boundaries," *Computers, Materials & Continua* 14(2009), 197-207.
10. M.A. Martorano, M.A. Fortes, A.F. Padilha, "The growth of protrusions at the boundary of a recrystallized grain," *Acta Mater.* 54(2006), 2769-2776.
11. M.A. Martorano et al., "Observations of grain boundary protrusions in static recrystallization of high-purity bcc metals," *Scripta Mater* 56(2007), 903-905.
12. R.B. Godiksen et al., "Simulations of boundary migration during recrystallization using molecular dynamics," *Acta Mater.* 55(2007), 6383-6391.
13. R.B. Godiksen, S. Schmidt, D. Juul Jensen, "Molecular dynamics simulations of grain boundary migration during recrystallization employing tilt and twist dislocation boundaries to provide the driving pressure," *Modeling Simul Mater Sci. Eng.* 16(2008), 065002.
14. S. Zaefferer, S.I. Wright, D. Raabe. "Three-Dimensional Orientation Microscopy in a Focused Ion Beam–Scanning Electron Microscope: A New Dimension of Microstructure Characterization," *Metal. Mater. Trans.* 39A(2007), 374-389.
15. M.D. Uchic et al., "Three-Dimensional Microstructural characterization Using Focused Ion Beam Tomography," *MRS Bulletin.* 32(2007), 408-416.
16. X. Huang, G. Winther, "Dislocation structures. Part I. Grain orientation dependence," Phil. *Mag.*, 87(2007), 5189-5214.
17. F.J. Humphreys, M. Hatherly, *Recrystallization and Related Annealing Phenomena, second ed.* (Pergamon Press, Oxford 2004).
18. G. Winther, X. Huang, "Dislocation structures. Part II. Slip system dependence," *Phil. Mag*. 87(2007), 5215-5235.
19. D. Juul Jensen, N. Hansen, "Flow stress anisotropy in aluminium," *Acta Metall. Mater.* 38(1990),1369-1380.
20. D. Juul Jensen, D.J. Rowenhorst, S. Schmidt, "Misorientation Aspects of Growth During Recrystallization," *Mater. Sci. Forum.* 558-559(2007), 85-92.